Journal of Hazardous Materials 295 (2015) 63–69

Contents lists available at ScienceDirect

Journal of Hazardous Materials

journal homepage: www.elsevier.com/locate/jhazmat

A regenerative electrochemical biosensor for mercury(II) by using the insertion approach and dual-hairpin-based amplification

Jia Jing[a], Ling Yu[a], Gao Zhong Feng[a], Lei Jing Lei[b], Luo Hong Qun[a,*], Li Nian Bing[a,*]

[a] Key Laboratory of Eco-Environments in Three Gorges Reservoir Region (Ministry of Education), School of Chemistry and Chemical Engineering, Southwest University, Chongqing 400715, PR China
[b] College of Chemistry and Chemical Engineering, Chongqing University, Chongqing 400044, PR China

HIGHLIGHTS

- The dual-hairpin structure as a signal amplifier is label-free and handy.
- The strategy uses the insertion approach to improve the hybridization efficiency.
- This biosensor has a low detection limit (28 pM) for detection of Hg^{2+}.
- This biosensor can be easily regenerated by using L-cysteine.

GRAPHICAL ABSTRACT

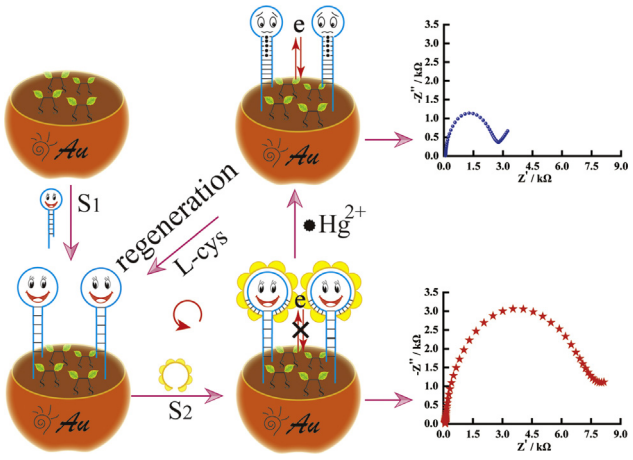

ARTICLE INFO

Article history:
Received 21 October 2014
Received in revised form 27 March 2015
Accepted 6 April 2015
Available online 8 April 2015

Keywords:
Label free
Insertion approach
Dual hairpin
Regeneration
Electrochemical impedance spectra

ABSTRACT

A simple and effective biosensor for Hg^{2+} determination was investigated. The novel biosensor was prepared by the insertion approach that the moiety-labeled DNA inserted into a loosely packed cyclic-dithiothreitol (DTT) monolayer, improving the hybridization efficiency. Electrochemical impedance spectroscopy studies of two biosensors (single-hairpin and dual-hairpin structure DNA modified electrodes) used for Hg^{2+} detection indicated that the dual-hairpin modified electrode had a larger electron transfer resistance change (ΔR_{ct}). Consequently, the dual-hairpin structure was used as a signal amplifier for the preparation of a selective Hg^{2+} biosensor. This biosensor exhibited an excellent selectivity toward Hg^{2+} over Cd^{2+}, Pd^{2+}, Co^{2+} etc. Also, a linear relation was observed between the ΔR_{ct} and Hg^{2+} concentrations in a range from 0.1 nM to 5 μM with a detection limit of 28 pM under optimum conditions. Moreover, the biosensor can be reused by using L-cysteine and successfully applied for detecting Hg^{2+} in real samples.

1. Introduction

Mercury ions (Hg^{2+}), toxicly accumulated in human bodies through the drinking water and food chains, will cause irreversible

* Corresponding authors. Tel.: +86 23 68253237; fax: +86 23 68253237.
E-mail addresses: luohq@swu.edu.cn (H.Q. Luo), linb@swu.edu.cn (N.B. Li).

http://dx.doi.org/10.1016/j.jhazmat.2015.04.017
0304-3894/

damage of gastrointestinal, neurologic and renal organ systems as well as other chronic diseases [1–4]. Due to the continuing concern over Hg^{2+} contamination on the environment and human health [5], it is highly desirable for sensitive and on-site detection of Hg^{2+} in disease prevention and environment protection.

It is well known that special T-T mismatches in DNA duplex show high selectivity for Hg^{2+} against other metal ions in aqueous solution to form T-Hg^{2+}-T base pairs [6]. The T-Hg^{2+}-T base pairs enable the single-stranded DNAs to fold into duplexes [7,8] and strengthen DNA duplexes [9,10]. This fact has stimulated the development of Hg^{2+} sensors based on colorimetric [11–13] and fluorescent methods [14–17], while others are based on polymermaterials [18,19], nanomaterials [20–23], DNAzymes [24–26], proteins [27–30]. They all show excellent performance. However, most of these sensors are time consuming and sophisticated synthesis of probe materials, in which case, developing new methods is necessary.

In the past decades, the self-assembly of DNA on gold electrodes employed the backfilling approach that alkanethiols were put into the void spaces between constituents of a pre-installed DNA monolayer [31]. Although this traditional method achieved the tremendous success, it lacked the reproducibility of electrochemical signals from DNA-modified electrodes [32]. Yang's group recently used the insertion method to improve the reproducibility and sensitivity of electrochemical signal [32]. Wang's group put forward a novel dual-hairpin DNA structure for ultrasensitive detection of Hg^{2+} with a detection limit of 52 pM [33], and his grounp also proposed a fast and sensitive strategy for the detection of targets based on dual-hairpin DNA structure [34]. Excellent selectivity and reliable results could be achieved but the problem of the labeled adjunct probe remains costly and complex synthesis procedure.

Here we report a sensitive, rapid, simple, and label-free electrochemical impedance spectroscopy (EIS) biosensor for detecting Hg^{2+} which is demonstrated by the insertion approach and the dual-hairpin structure, resulting in improvements in economy and repeatability. A linear relationship between the logarithmic value of the Hg^{2+} concentration and the change in the electron transfer resistance (ΔR_{ct}, $\Delta R_{ct} = R_{ct}^0 - R_{ct}$, and R_{ct}^0 and R_{ct} represent the interfacial electron transfer resistance value of the dual-hairpin DNA modified biosensor in the absence and presence of Hg^{2+}, respectively.) is in the range from 0.1 nM to 5 μM, and a detection limit of 28 pM is obtained.

2. Material and methods

2.1. Chemicals and reagents

Dithiothreitol (DTT), L-cysteine (L-Cys), HPLC-purified capture probe (S_1), and adjunct DNA (S_2) were purchased from Sangon

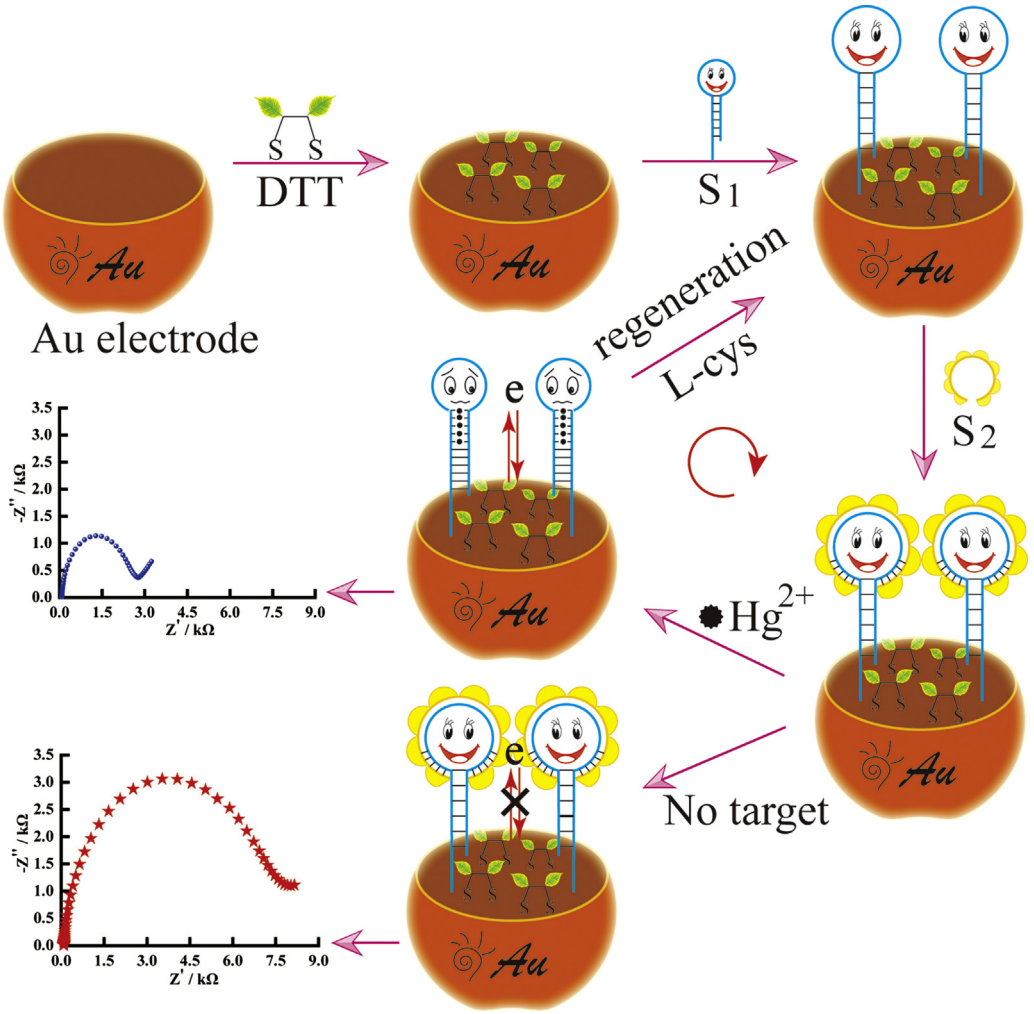

Scheme 1. Schematic illustration of the detection of Hg^{2+} based on electrochemical signal amplification by dual-hairpin DNA structure in combination with the insertion approach.

Biotechnology Co., Ltd. (Shanghai, China) and DNA sequences are shown below:

S_1: 3′-HS-$(CH_2)_6$-CGGCGGTTTTTAGGAGAGTTTTTCCGCCG-5′

S_2: 3′-AAAAAGAAGGGAGTGGAAGGAGAAAAA-5′

Tris (2-carboxyethyl) phosphine hydrochloride (TCEP) and 6-mercapto-1-hexanol (MCH) were purchased from Sigma Chemical Co. (St. Louis, MO, USA). All the reagents mentioned were analytical reagent grades and used without further purification. Ultrapure water (specific resistance of 18.2 MΩ cm) was used throughout the experiments. The buffer solutions used in this work were listed as follows:

C-buffer (pH 7.4) contains 100 mM Tris-HCl, 0.1 M NaCl, and 5 mM $MgCl_2$. I-buffer (pH 7.4) contains 10 mM Tris-HCl, 20 mM TCEP, and 1 M NaCl. D-buffer (pH 7.4) contains 10 mM Tris-HCl and 1 M NaCl. H-buffer (pH 7.4) contains 10 mM phosphate buffer solution (PBS) and 300 mM NaCl. W-buffer (pH 7.4) is 10 mM Tris-HCl.

2.2. Apparatus

All electrochemical measurements were monitored on an electrochemical workstation (CHI 660D, CH Instruments, Chenhua Corp, Shanghai, China) at room temperature. The experiment was performed with a typical three electrode system, in which the working electrode was the functionalized gold electrode, the reference electrode was an Ag/AgCl electrode with saturated KCl, and the counter electrode was a platinum electrode. Ferricyanide solution (5.0 mM $[Fe(CN)_6]^{3-/4-}$) used as the supporting electrolyte medium was obtained by dissolving potassium ferrocyanide and potassium ferricyanide with PBS (0.1 M, pH 7.4), and the concentrations of potassium ferrocyanide and potassium ferricyanide are 2.5 mM, respectively. Cyclic voltammetry (CV) was performed within the potential range from −0.3 to 0.7 V at 0.1 V s^{-1}. Electrochemical impedance spectra (EIS) were performed in a frequency range from 0.1 Hz to 10 kHz with 5 mV as the amplitude.

2.3. Electrode pretreatment

The gold electrode (4.0 mm in diameter) was polished carefully with alumina powder (1.0, 0.3, and 0.05 μm in diameter) on a microcloth pad in sequence until a mirror surface was formed, followed by ultrasonic cleaning with ultrapure water, ethanol, and ultrapure water for 5 min each to remove the residual Al_2O_3 powder. The above electrode was electrochemically cleaned by cycling the potential between −0.2 and +1.6 V (vs. Ag/AgCl) at 0.1 V s^{-1} in a 0.5 M H_2SO_4 solution until a steady-state redox wave was obtained. Finally, the prepared electrode was rinsed with ultrapure water and dried with nitrogen.

2.4. Sensor preparation

Before use, the capture probe S_1 was dissolved in D-buffer and stored at 4 °C over night. The probe S_1 solution was heated at 90 °C for 5 min, followed by slowly cooling down to room temperature [34]. To ensure the absence of probe dimers, the above S_1 probe solution was diluted by mixing 2.0 μM S_1 probe with I-buffer with the same volume for 1 h in the dark [32].

For the insertion approach, the cleaned electrode was first immersed in 25 μL of 200 μM freshly prepared DTT solution (dissolved in D-buffer) for 10 min, and then the DTT modified electrode was immersed in 25 μL of 1.0 μM S_1 for 10 h at room temperature. The prepared electrode was incubated with 2.5 μM S_2 probe in H-buffer for 3 h at 37 °C to form the dual-hairpin structure.

For the traditional backfilling method, the cleaned electrode was immersed in 25 μL of 1.0 μM S_1 solution for 10 h at room temperature, followed a incubation progress in 25 μL of 2 mM MCH for 2 h. Next, the S_1 modified electrode was hybridized with S_2 (25 μL, 2.5 μM) for 3 h at 37 °C to obtain the final dual-hairpin DNA modified biosensor. The electrode was thoroughly rinsed with W-buffer after each step throughout the experimental process.

2.5. Detection of Hg^{2+} with the dual-hairpin structure DNA

According to the references [7,32,35], T bases can complete the reaction with Hg^{2+} in one hour in the solution. Thus, the reaction time between T bases and Hg^{2+} in this experiment was 1 h. For the Hg^{2+} detection, the prepared biosensors were then immersed in 100 μL of H-buffer containing different concentrations of Hg^{2+} for 1 h at room temperature to form T-Hg^{2+}-T complex. In order to ensure that the system can reach stable state and obtain an accurate value of R_{ct}, the electrode was soaked in $[Fe(CN)_6]^{3-/4-}$ solution for 3 min before each EIS measurement [36].

3. Results and discussion

3.1. Designed sensing system for Hg^{2+} detection

It is well known that DTT could be chemisorbed onto the gold electrode via Au-S bonds, which two hydroxyl groups are exposed at the outer surface, to form a compact surface with the cyclic-(DTT) configuration backfillers [37]. The cyclic-(DTT) configuration backfillers could provide enough free space around the hairpin structure DNA S_1 to ensure the subsequent assembly, so the formation of dual-hairpin structure becomes much easier.

In order to explore whether the DTT modified on the electrode has effect on the Hg^{2+} detection in the experiments or not, the control experiment of the DTT / Au electrode in the absence and presence of Hg^{2+} has been conducted. By analyzing the experimental results, we have found that the DTT modified on Au electrode has almost no interference in the Hg^{2+} detection (see Supporting Information for details).

Scheme 1 illustrates the working mechanism of Hg^{2+} detection based on electrochemical signal amplification by dual-hairpin DNA structure in combination with the insertion approach. First, the DTT could be stabilized by Au-S bonding to form a uniform monomolecular layer on the gold electrode. The thiol moiety-labeled and T-rich hairpin structure DNA S_1, designed with 6 complementary base pairs in the stem region, could insert into the preassembled DTT monolayer. The adjunct DNA S_2 can be easily captured by the immobilized S_1 to form the dual-hairpin structure because of ten base pairs of S_2 matching with S_1 in the loop region. The electron transfer between gold surface and $[Fe(CN)_6]^{3-/4-}$ electrolyte solution is hindered to present a higher R_{ct}, due to the highly negatively charged oligonucleotides skeleton. The S_1 probe contains 5 special T-T mismatches that have high affinity with the Hg^{2+}, generating T-Hg^{2+}-T complexes. The exact base pairing graph of the conformation switches between the dual-hairpin DNA and the single-hairpin DNA in the presence of Hg^{2+} is illustrated in Fig. S2 in the Supporting Information. As T-Hg^{2+}-T base pairs are much more stable than natural A-T base pairs [38], the loop of S_1 shrinks and S_2 separates from the biosensor surface, presenting a low R_{ct} value. Thus, a novel biosensor used to detect Hg^{2+} could be developed based on ΔR_{ct}.

3.2. Characterization of assembly on the electrode

As is known, EIS is an effective tool to characterize the fabrication process of the proposed sensor [39]. The diameter of the semicircle portion corresponds to the R_{ct} and the increase of the diameter reflects the increase of the interfacial R_{ct} [40]. As shown in Fig. 1A, the R_{ct} increased substantially with the modification of DTT (curve b), S_1 (curve c), and S_2 (curve d) to the Au electrode surface in sequence. The equivalent circuit (Table S1) was used to fit the EIS data which includes the solution resistance (R_s), the constant phase

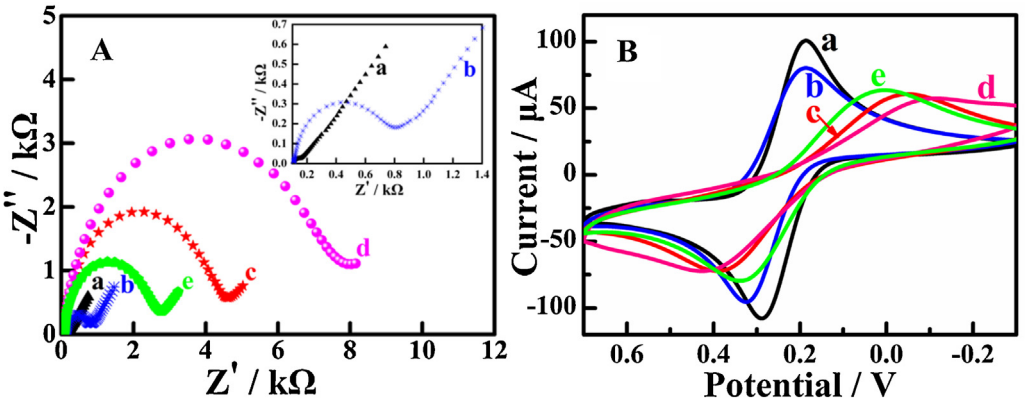

Fig. 1. (A) Nyquist diagrams and (B) cyclic voltammograms of the biosensor at different stages: bare Au (a), DTT / Au (b), S_1 / DTT / Au (c), S_2 / S_1 / DTT / Au (d), and S_2 / S_1 / DTT / Au in the presense of 5 μM Hg^{2+} (e).

element (CPE) related to double layer capacitance, charge transfer resistance (R_{ct}), and the Warburg impedance (Z_w) [41]. The calculated R_{ct} values are shown in Table S1, it can be seen that the bare gold electrode shows a tiny R_{ct} value (48.8 Ω), indicating a rapid electron transfer process of $[Fe(CN)_6]^{3-/4-}$. The immobilization of the DTT monolayer led to an increased R_{ct} value (643.2 Ω), then, the insert-assembly of a thiolated S_1 monolayer resulted in a larger R_{ct} value (4143 Ω), because the formation of the hairpin structure of S_1 hindered the interfacial electron transfer. With the treatment of S_2, a much larger R_{ct} value (7031 Ω) was observed, because S_2 increased the density of negative charges on the electrode surface and the electrostatic repulsion between DNA and redox probe. The changes of EIS plots proved the dual-hairpin structure successfully formed on the gold electrode [34]. The DNA area percentage on the gold electrode surface (θ) was calculated to be 90.85 % (see Supporting Information for details). A high R_{ct} intensity corresponds to a big θ value. This phenomenon can be explained by the formation of dual-hairpin structure mentioned above. After the addition of Hg^{2+} (curve e, Fig. 1A), the R_{ct} value declined obviously (2443 Ω, Table S1), this is because the T-Hg^{2+}-T conformation induced the loops of S_1 of dual-hairpin structure to shrink, and the negatively charged S_2 separated from the electrode surface. These two aspects were beneficial for electron transfer between gold surface and $[Fe(CN)_6]^{3-/4-}$ electrolyte solution. The above results coincided with the presumptive mechanism of the electrochemical biosensor that the Hg^{2+}-induced conformation switch of dual-hairpin to single-hairpin structure.

Fig. 1B shows the CVs of the gold electrode at different modification steps. As displayed in Fig. 1B, an increase in the peak to peak separation (ΔE) and decrease in the peak current was accompanied with the stepwise modification of DTT, S_1, and S_2 on the gold electrode, which could be attributed to the obstruction of the interfacial electron transfer caused by the formation of compact monolayer including DTT and negatively charged S_1 and S_2. However, the peak current increased and the ΔE decreased with the addition of Hg^{2+}. The CVs results coincided with the observations of the EIS experiments, which further proved the changes in the structure of DNA on the electrode surface.

3.3. Advantage of the insertion approach with dithiothreitol versus backfilling method and signal amplification of the dual-hairpin structure DNA

In order to verify that the first assembled DTT can improve the hybridization efficiency of S_1 and S_2, we investigated ΔR_{ct} responses (ΔR_{ct} (1)) of the backfilling method and the insertion approach preparing single-hairpin modified biosensors before and after hybridization with 2.5 μM S_2, respectively. For the traditional backfilling method, S_1, MCH, and S_2 were assembled on the cleaned electrode surface in sequence for preparing the biosensor. As shown in Fig. 2A and B, the ΔR_{ct} (1) of the backfilling method is much smaller than that of the insertion approach (inset, Fig. 2A). This is because when S_1 was first assembled on the electrode surface, the S_1 probes would be in a high density and the inter-probe distance among the S_1 probes in the monolayer became inhomogeneous [32]. Thus, it would interfere with the subsequent hybridization between S_1 and S_2, leading to few quantity of dual-structure DNAs. Consequently, the signal amplification of the backfilling method is weak. But for the insert approach, the cyclic-(DTT) configuration backfillers provided enough free space around S_1 to allow the subsequent assembly of S_2, resulting in the obvious improvement of hybridization efficiency between S_1 and S_2. Therefore, the number of dual-hairpin structure DNA on the electrode surface would be increased. In conclusion, the insertion approach can replace the backfilling method in the experiment to improve the hybridization efficiency of S_1 and S_2.

Signal amplification is necessary for building a highly sensitive biosensor. To demonstrate the enhancement of electrochemical signal of the dual-hairpin structure, we investigated ΔR_{ct} responses (ΔR_{ct} (2)) of S_1 / DTT and S_2 / S_1 / DTT biosensors for Hg^{2+} detection. As shown in Fig. 2C and D, the ΔR_{ct} (2) values of the two biosensors in the absence and presence of Hg^{2+} were compared. The ΔR_{ct} (2) of S_1 / DTT / Au was 1766 Ω, while the ΔR_{ct} (2) value of S_2 / S_1 / DTT / Au was 4588 Ω which is much higher than that of S_1 / DTT / Au. This is because the dual-hairpin structure has more negatively charged oligonucleotides skeleton than single-hairpin structure, presenting larger interfacial electron transfer resistance on the electrode surface. In the presence of Hg^{2+}, the dual-hairpin structure contributes to the ΔR_{ct} in two ways, one is the loops of inter-hairpins S_1 shrank, and the other is the negatively charged DNA S_2 separated from the electrode surface. However, the single-hairpin structure only contributes to the shrink of the loop. This result indicates that the dual-hairpin structure could amplify the signal distinctly at the same concentration of Hg^{2+}.

Furthermore, the repeatability of the sensor was explored by monitoring the R_{ct} signal in 100 nM Hg^{2+} solution for 3 replicate determinations under same conditions (Fig. S3, Supporting Information). As a result, the dual-hairpin biosensor possesses a good repeatability.

3.4. Sensitivity of the biosensor

In order to obtain the optimum conditions, the effect of experimental conditions was investigated. Fig. S4 shows four variables

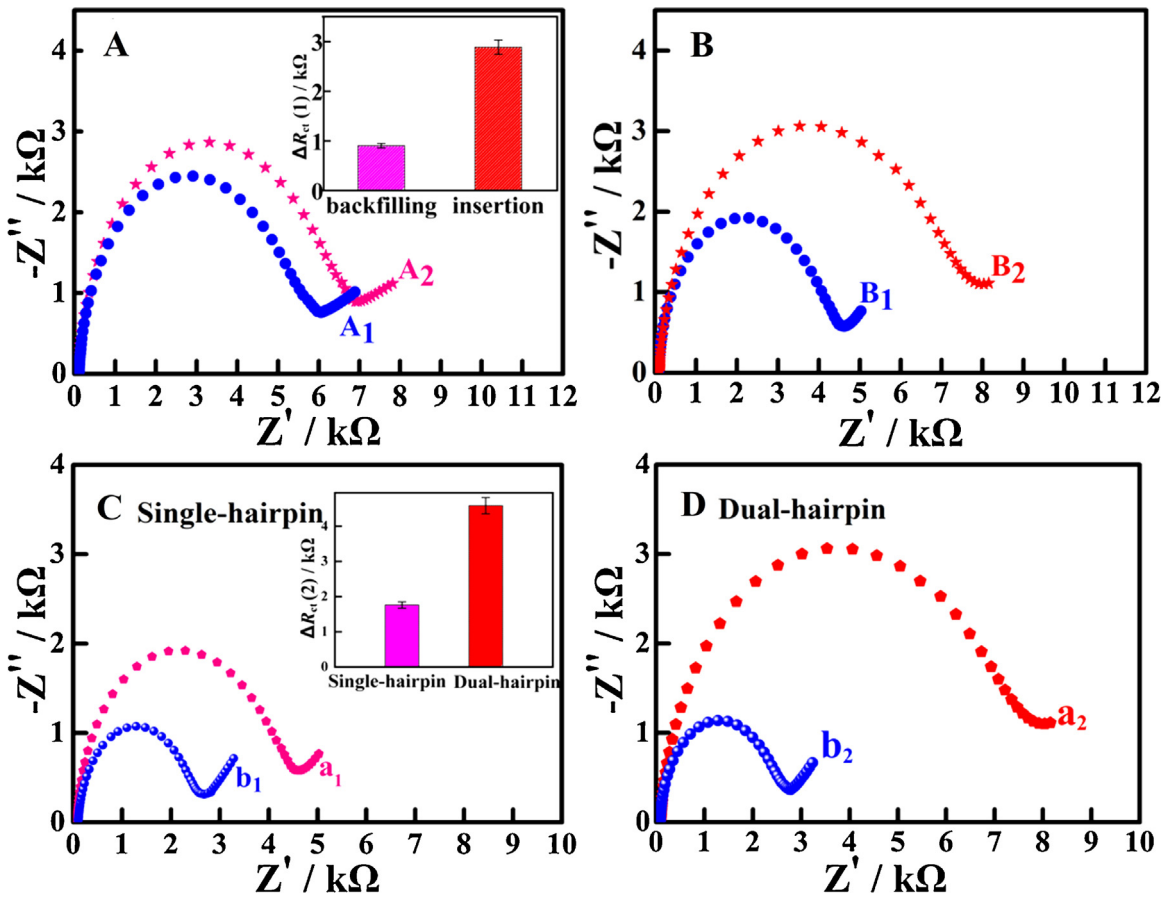

Fig. 2. Nyquist diagrams of the backfilling approach (A) and the insertion approach (B), respectively: MCH / S_1 / Au (A_1, Fig. 2A) and S_2 / MCH / S_1 / Au (A_2, Fig. 2A), S_1 / DTT / Au (B_1, Fig. 2B), and S_2 / S_1 / DTT / Au (B_2, Fig. 2B). Inset (Fig. 2A): The comparison of $\Delta R_{ct}(1)$ of the backfilling method and the insertion approach preparing single-hairpin modified biosensors before and after hybridization with 2.5 μM S_2. Nyquist diagrams of the single-hairpin and dual-hairpin structure modified biosensors in the absence and presence of Hg^{2+} (1 μM): S_1 / DTT / Au in the absence of Hg^{2+} (a1, Fig. 2C) and in the presence of Hg^{2+} (b1, Fig. 2C), S_2 / S_1 / DTT / Au in the absence of Hg^{2+} (a2, Fig. 2D) and in the presence of Hg^{2+} (b2, Fig. 2D). Inset (Fig. 2C): The comparison of ΔR_{ct} (2) between the single-hairpin and the dual-hairpin structure modified biosensors in the absence and presence of Hg^{2+}.

of the system including the effect of pH, the concentration of DTT and S_2, and the hybridization time. It is obvious that the ΔR_{ct} response to Hg^{2+} was influenced by solution acidity significantly (Fig. S4B). The ΔR_{ct} was low below pH 5.0 but increased rapidly with the increase of pH; over pH 6.5, the increase is relatively low and the ΔR_{ct} approached the maximum at pH 7.4; after that, the ΔR_{ct} decreased. The reason for the influence of pH on T–Hg^{2+}–T interaction may be that at a pH below 5.0, protonation of the nitrogen atoms of the thymine base reduces its affinity with Hg^{2+}, while at a relatively higher pH, Hg^{2+} may be complexed by OH−, which in turn, reduces its complex with thymine bases. The experimental results showed that the optimum pH of the system is 7.4. The concentrations of DTT and S_2 were 200 μM and 2.5 μM, and the hybridization time of 3 h were chosen as optimum experimental conditions (see Supporting information for details).

Under optimum conditions, EIS measurements of Hg^{2+} at various concentrations were used to determine dynamic range and detection limit of the proposed biosensor. Typical Nyquist plots of the biosensor incubated with different concentrations of Hg^{2+} are shown in Fig. 3. The ΔR_{ct} against the logarithm of Hg^{2+} concentration was linear (Fig. 3, inset) over the range from 0.1 nM to 5 μM ($\Delta R_{ct} = 10.328 + 0.962 \times \log C$ (M)) with a detection limit of 28 pM based on a signal three-fold the background noise. Such a low detection limit is much lower than the US Environmental Protection Agency (EPA) standard (10 nM of Hg^{2+} for drinkable water).

The methods recently developed for Hg^{2+} detection are listed in Table S2. Most designs of these methods involve nanometer

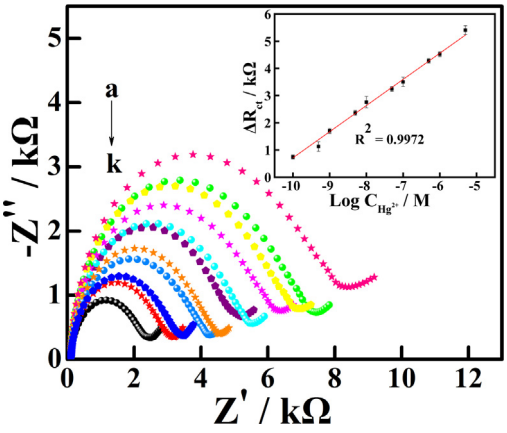

Fig. 3. Nyquist diagrams for the biosensor immersed in different concentrations of Hg^{2+} (a–k): (a) blank (0 nM), (b) 0.1 nM, (c) 0.5 nM, (d) 1 nM, (e) 5 nM, (f) 10 nM, (g) 50 nM, (h) 100 nM, (i) 500 nM, (j) 1 μM, and (k) 5 μM. Inset: the resulting calibration curve of ΔR_{ct} (1) for the target Hg^{2+} over the range of 0.1 nM–5 μM. Error bars represent the standard deviation of three replicates from one electrode.

materials, which are costly and time-consuming. In addition, the detection limits of most of these methods are not so low. Compared to these methods, our sensor has the advantage of easy operation with a relatively low detection limit. Moreover, our sensor can be easily regenerated and exhibits good repeatability.

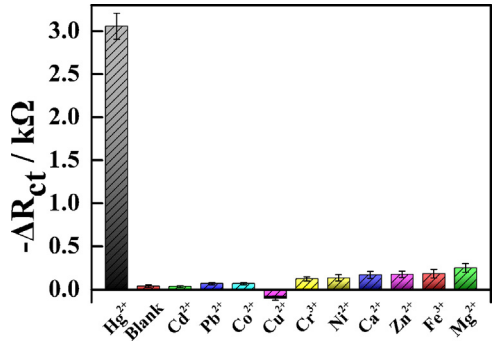

Fig. 4. Selectivity of the biosensor for Hg^{2+} determination. The concentration of all interfering metal ions was 1 μM, and that of Hg^{2+} was 100 nM.

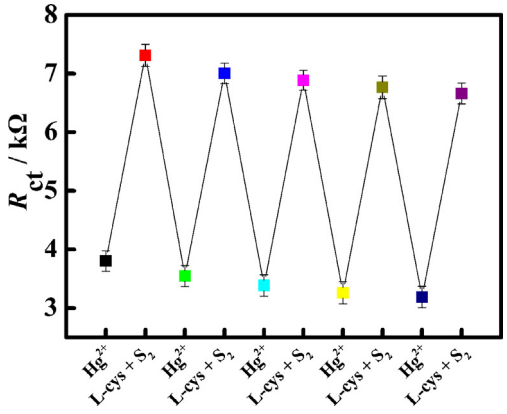

Fig. 5. Reversible changes of the R_{ct} of the dual-hairpin biosensor when immersed in the solution of 100 nM Hg^{2+} ions, 1.0 mM L-cysteine, and 2.5 μM S_2, alternately.

3.5. Selectivity of the biosensor

To investigate the selectivity of our proposed sensing system, we tested a series of commonly existing metal ions, including Cd^{2+}, Pb^{2+}, Co^{2+}, Cu^{2+}, Cr^{3+}, Ni^{2+}, Ca^{2+}, Zn^{2+}, Fe^{3+}, and Mg^{2+} (each 1 μM) under optimum conditions. Fig. 4 depicts the ΔR_{ct} responses of the biosensors to various metal ions. As expected, even micromole concentrations of typical metal ions exhibit much weaker ΔR_{ct} responses than Hg^{2+} at nM level. Therefore, our Hg^{2+} detection method has an excellent selectivity for Hg^{2+} against other environmentally relevant metal ions. The good performance in selectivity is mainly attributed to the specific coordination between T bases and Hg^{2+}.

3.6. Practical application

To evaluate whether this biosensor is applicable to natural samples, the recoveries of added Hg^{2+} in water sample from Jialing River were determined. The water samples added with Hg^{2+} at three different concentrations of 1, 100, and 5000 nM were tested. The results are listed in Table S3, the recovery of Hg^{2+} in the range of 98.8–104% was achieved, which demonstrated the feasibility of this method in real samples.

3.7. Reusability of the biosensor

For a biosensor, the reusability is an important factor for practical application. Here, L-cysteine was employed to remove Hg^{2+} from the T–Hg^{2+}–T complexes [42], resulting in the regeneration of the single hairpin structure of S_1. So the S_1 could be hybridized with S_2 to reform dual-hairpin structure on the electrode surface again, therefore, the dual-hairpin biosensor could be reused conveniently. In general, after reaction with Hg^{2+}, the biosensor was immersed in the L-cysteine solution (1.0 mM) for 1 h at room temperature, followed by rinsing with ultrapure water and drying by nitrogen. The Hg^{2+} of T–Hg^{2+}–T complexes could be removed and the hairpin structure of S_1 recovered to the original state. Fig. 5 shows the R_{ct} of the dual-hairpin biosensor immersed alternately in the solutions of 100 nM Hg^{2+}, 1 mM L-cysteine, and 2.5 μM S_2 for five regeneration cycles. It can be seen that the R_{ct} changed reversibly, which can be ascribed to the reversible transformation between the single-hairpin structure and the dual-hairpin structure of the biosensor. Moreover, this biosensor almost retained its original performance after five regeneration cycles. It is consistent with the literature that the L-cysteine does not affect the response and repeatability of the Hg^{2+} biosensor [43,44]. As a result, the prepared dual-hairpin biosensor coubld be reused to detect Hg^{2+}.

4. Conclusions

In summary, an efficient and label-free biosensor for Hg^{2+} detection by combining the insertion approach with a dual-hairpin structure was demonstrated. Compared to the conventional labeling technology-based sensor, the label-free strategy is much simple and efficient. Moreover, the prepared biosensor can detect Hg^{2+} in a low concentration (28 pM) with negligible response to other metal ions and can be easily regenerated by removing Hg^{2+} from T-Hg^{2+}-T base pairs by using L-cysteine. In view of these merits, the same approach can be applied to other objects in aqueous solutions.

Acknowledgments

This work was financially supported by the National Natural Science Foundation of China (No. 21273174) and the Municipal Science Foundation of Chongqing City (No. CSTC–2013jjB00002).

Appendix A. Supplementary data

Supplementary data associated with this article can be found, in the online version, at http://dx.doi.org/10.1016/j.jhazmat.2015.04.017.

References

[1] M.L.A. Cuvin-Aralar, R.W. Furness, Mercury and selenium interaction: a review, Ecotoxicol. Environ. Saf. 21 (1991) 348–364.
[2] P.B. Tchounwou, W.K. Ayensu, N. Ninashvili, D. Sutton, Environmental exposure to mercury and its toxicopathologic implications for public health, Environ. Toxicol. 18 (2003) 149–175.
[3] M. Gochfeld, Cases of mercury exposure, bioavailability, and absorption, Ecotoxicol. Environ. Saf. 56 (2003) 174–179.
[4] A. Sari, M. Tuzen, Removal of mercury(II) from aqueous solution using moss (drepanocladus revolvens) biomass: equilibrium, thermodynamic and kinetic studies, J. Hazard. Mater. 171 (2009) 500–507.
[5] K. Alizadeh, R. Parooia, P. Hashemi, B. Rezaei, M.R. Ganjali, A new schiff's base ligand immobilized agarose membrane optical sensor for selective monitoring of mercury ion, J. Hazard. Mater. 186 (2011) 1794–1800.
[6] S.F. Xu, L.X. Chen, J.H. Li, Y.F. Guan, H.Z. Lu, Novel Hg^{2+}-imprinted polymers based on thymine-Hg^{2+}-thymine interaction for highly selective preconcentration of Hg^{2+} in water samples, J. Hazard. Mater. 237–238 (2012) 347–354.
[7] F. Xuan, X. Luo, I.M. Hsing, Conformation-dependent exonuclease III activity mediated by metal ions reshuffling on thymine-rich DNA duplexes for an ultrasensitive electrochemical method for Hg^{2+} detection, Anal. Chem. 85 (2013) 4586–4593.
[8] R. Freeman, T. Finder, I. Willner, Multiplexed analysis of Hg^{2+} and Ag^{+} ions by nucleic acid functionalized CdSe/ZnS quantum dots and their use for logic gate operations, Angew. Chem. Int. Ed. 48 (2009) 7818–7821.
[9] Z.Q. Zhu, Y.Y. Su, J. Li, D. Li, J. Zhang, S.P. Song, Y. Zhao, G.X. Li, C.H. Fan, Highly sensitive electrochemical sensor for mercury(II) ions by using a mercury-specific oligonucleotide probe and gold nanoparticle-based amplification, Anal. Chem. 81 (2009) 7660–7666.

[10] J.-S. Lee, C.A. Mirkin, Chip-based scanometric detection of mercuric ion using DNA-functionalized gold nanoparticles, Anal. Chem. 80 (2008) 6805–6808.
[11] T. Li, S.J. Dong, E.K. Wang, Label-free colorimetric detection of aqueous mercury ion (Hg^{2+}) using Hg^{2+}-modulated G-quadruplex-based DNAzymes, Anal. Chem. 81 (2009) 2144–2149.
[12] R. Shunmugam, G.J. Gabriel, C.E. Smith, K.A. Aamer, G.N. Tew, A highly selective colorimetric aqueous sensor for mercury, Chem. Eur. J. 14 (2008) 3904–3907.
[13] Y. Bhattacharjee, A. Chakraborty, Label-free cysteamine-capped silver nanoparticle-based colorimetric assay for Hg(II) detection in water with subnanomolar exactitude, ACS Sustain. Chem. Eng. 2 (2014) 2149–2154.
[14] H. Wang, Y.X. Wang, J.Y. Jin, R.H. Yang, Gold nanoparticle-based colorimetric and turn-on fluorescent probe for mercury(II) ions in aqueous solution, Anal. Chem. 80 (2008) 9021–9028.
[15] C.C. Huang, Z. Yang, K.H. Lee, H.T. Chang, Synthesis of highly fluorescent gold nanoparticles for sensing mercury(II), Angew. Chem. 119 (2007) 6948–6952.
[16] B. Liu, H. Tian, A selective fluorescent ratiometric chemodosimeter for mercury ion, Chem. Commun. (2005) 3156–3158.
[17] R. Meítivier, I. Leray, B. Valeur, Lead and mercury sensing by calixarene-based fluoroionophores bearing two or four dansyl fluorophores, Chem. Eur. J. 10 (2004) 4480–4490.
[18] G.G. Talanova, N.S.A. Elkarim, V.S. Talanov, R.A. Bartsch, A calixarene-based fluorogenic reagent for selective mercury(II) recognition, Anal. Chem. 71 (1999) 3106–3109.
[19] Y. Cho, S.S. Lee, J.H. Jung, Recyclable fluorimetric and colorimetric mercury-specific sensor using porphyrin-functionalized $Au@SiO_2$ core/shell nanoparticles, Analyst 135 (2010) 1551–1555.
[20] N. Zhang, G. Li, Z.H. Cheng, X.J. Zuo, Rhodamine B immobilized on hollow Au–HMS material for naked-eye detection of Hg^{2+} in aqueous media, J. Hazard. Mater. 229–230 (2012) 404–410.
[21] H. Khania, M.K. Rofouei, P. Arab, V.K. Gupta, Z. Vafaei, Multi-walled carbon nanotubes-ionic liquid-carbon paste electrode as a super selectivity sensor: application to potentiometric monitoring of mercury ion(II), J. Hazard. Mater. 183 (2010) 402–409.
[22] I. Chakraborty, T. Udayabhaskararao, T. Pradeep, Luminescent sub-nanometer clusters for metal ion sensing: a new direction in nanosensors, J. Hazard. Mater. 211–212 (2012) 396–403.
[23] S.H. Chen, D.B. Liu, Z.H. Wang, X.L. Sun, D.X. Cui, X.Y. Chen, Picomolar detection of mercuric ions by means of gold–silver core–shell nanorods, Nanoscale 5 (2013) 6731–6735.
[24] J.W. Liu, Y. Lu, Rational design of Turn-On allosteric DNAzyme catalytic beacons for aqueous mercury ions with ultra high sensitivity and selectivity, Angew. Chem. 119 (2007) 7731–7734.
[25] J.M. Thomas, R. Ting, D.M. Perrin, Label-free colorimetric detection of aqueous mercury ion (Hg^{2+}) using Hg^{2+}-modulated G-quadruplex-based DNAzymes, Org. Biomol. Chem. 2 (2004) 307–312.
[26] M. Hollenstein, C. Hipolito, C. Lam, D. Dietrich, D.M. Perrin, A highly selective DNAzyme sensor for mercuric ions, Angew. Chem. Int. Ed. 47 (2008) 4346–4350.
[27] I.-B. Kim, U.H.F. Bunz, Modulating the sensory response of a conjugated polymer by proteins: an agglutination assay for mercury ions in water, J. Am. Chem. Soc. 128 (2006) 2818–2819.
[28] B.R. White, H.M. Liljestrand, J.A. Holcombe, A 'turn-on' FRET peptide sensor based on the mercury binding protein MerP, Analyst 133 (2008) 65–70.
[29] S. Cherian, R.K. Gupta, B.C. Mullin, T. Thundat, Detection of heavy metal ions using protein-functionalized microcantilever sensors, Biosens. Bioelectron. 19 (2003) 411–416.
[30] Z. Gu, M.X. Zhao, Y.W. Sheng, L.A. Bentolila, Y. Tang, Detection of mercury ion by infrared fluorescent protein and its hydrogel-based paper assay, Anal. Chem. 83 (2011) 2324–2329.
[31] T.M. Herne, M.J. Tarlov, Characterization of DNA probes immobilized on gold surfaces, J. Am. Chem. Soc. 119 (1997) 8916–8920.
[32] L. Yang, C.H. Zhang, H. Jiang, G.J. Li, J.H. Wang, E.K. Wang, The insertion approach: bolstering the reproducibility of electrochemical signal amplification via DNA superstructures, Anal. Chem. 86 (2014) 4657–4662.
[33] G.F. Wang, H. Huang, X.J. Zhang, L. Wang, Electrically contacted enzyme based on dual hairpin DNA structure and its application for amplified detection of Hg^{2+}, Biosens. Bioelectron. 35 (2012) 108–114.
[34] X.P. He, G.F. Wang, G. Xu, Y.H. Zhu, L. Chen, X.J. Zhang, A simple, fast, and sensitive assay for the detection of DNA, thrombin, and adenosine triphosphate based on dual-hairpin DNA structure, Langmuir 29 (2013) 14328–14334.
[35] Z.P. Zhang, J.G. Yin, Z.Y. Wu, R.Q. Yu, Electrocatalytic assay of mercury(II) ions using a bifunctional oligonucleotide signal probe, Anal. Chim. Acta 762 (2013) 47–53.
[36] X.Y. Zhang, L.Y. Zhou, H.Q. Luo, N.B. Li, A sensitive and label-free impedimetric biosensor based on an adjunct probe, Anal. Chim. Acta 776 (2013) 11–16.
[37] Y.T. Wang, J.J. Feng, Z.A. Tan, H.Y. Wang, Electrochemical impedance spectroscopy aptasensor for ultrasensitive detection of adenosine with dual backfillers, Biosens. Bioelectron. 60 (2014) 218–223.
[38] D.W. Huang, C.G. Niu, X.Y. Wang, X.X. Lv, G.M. Zeng, Turn-On fluorescent sensor for Hg^{2+} based on single-stranded DNA functionalized Mn:CdS/ZnS quantum dots and gold nanoparticles by time-gated mode, Anal. Chem. 85 (2013) 1164–1170.
[39] I.I. Suni, Impedance methods for electrochemical sensors using nanomaterials, TrAC Trends Anal. Chem. 27 (2008) 604–611.
[40] J.B. Raoof, M.S. Hejazi, R. Ojani, E.H. Asl, A comparative study of carbon nanotube paste electrode for development of indicator-free DNA sensors using DPV and EIS: human interleukin-2 oligonucleotide as a model, Int. J. Electrochem. Sci. 4 (2009) 1436–1451.
[41] D.H. Wu, Q. Zhang, X. Chu, H.B. Wang, G.L. Shen, R.Q. Yu, Ultrasensitive electrochemical sensor for mercury(II) based on target-induced structure-switching DNA, Biosens. Bioelectron. 25 (2010) 1025–1031.
[42] Y.Q. Zhang, L.J. Gao, L.P. Wen, L.P. Heng, Y.L. Song, Highly sensitive, selective and reusable mercury(II) ion sensor based on a ssDNA-functionalized photonic crystal film, Phys. Chem. Chem. Phys. 15 (2013) 11943–11949.
[43] D. Han, Y.-R. Kim, J.-W. Oh, T.H. Kim, R.K. Mahajan, J.S. Kim, H. Kim, A regenerative electrochemical sensor based on oligonucleotide for the elective determination of mercury(II), Analyst 134 (2009) 1857–1862.
[44] J.S. Lee, P.A. Ulmann, M.S. Han, C.A. Mirkin, A DNA-gold nanoparticle-based colorimetric competition assay for the detection of cysteine, Nano Lett. 8 (2008) 529–533.